Structural Engineering and Mechanics, Vol. 17, No. 5 (2004) 641-654
DOI: http://dx.doi.org/10.12989/sem.2004.17.5.641

An analytical solution for static analysis of a simply supported moderately thick sandwich piezoelectric plate

Lanhe Wu†, Zhiqing Jiang† and Wenjie Feng†

Department of Mechanics and Engineering Science, Shijiazhuang Railway Institute, Shijiazhuang 050043, P.R. China

(Received March 6, 2003, Accepted November 6, 2003)

Abstract. This paper presents a theoretic model of a smart structure, a transversely isotropic piezoelectric thick square plate constructed with three laminas, piezoelectric-elastic-piezoelectric layer, by adopting the first order shear deformation plate theory and piezoelectric theory. This model assumes that the transverse displacements through thickness are linear, and the in-plane displacements in the mid-plane of the plate are not taken to be account. By using Fourier's series expansion, an exact Navier typed analytical solution for deflection and electric potential of the simply supported smart plate is obtained. The electric boundary conditions are being grounded along four vertical edges. The external voltage and non-external voltage applied on the surfaces of piezoelectric layers are all considered. The convergence of the present approach is carefully studied. Comparison studies are also made for verifying the accuracy and the applicability of the present method. Then some new results of the electric potentials and displacements are provided. Numerical results show that the electrostatic voltage is approximately linear in the thickness direction, while parabolic in the plate in-plane directions, for both the deflection and the electric voltage. These results are very useful for distributed sensing and finite element verification.

Key words: sandwich plate; piezoelectric plate; piezoelectric material; first order shear deformation theory; analytical solution; bending.

1. Introduction

The study of embedded or surface mounted piezoelectric materials in structures has received considerable attention in recent years. One reason for this is that it may be possible to create certain types of structures and systems capable of adapting to or correcting for changing operating conditions. The advantage of incorporating these special types of material into the structure is that the sensing and actuating mechanism becomes part of the structure by sensing and actuating strains directly. These types of mechanism are referred to as strain sensing and actuating. This advantage is especially apparent for structures that are deployed in space. Generally space borne structures are very flexible because they are not designed for operations in which the force of gravity is present. In addition, they are characterized as having very low level of damping. Thus, transient vibrations

† Professor

endure for longer periods of time than is acceptable and operations may be interrupted. Proof-mass actuators, thrusters, and piezoelectric materials as described here are possible means of controlling the vibrations. Of course, there may also be many other good methods that have not as yet been thought of. However, generally speaking, most actuator systems other than the strain induced type add a considerable amount of weight and a possible space to the structure, thereby changing its mechanical properties significantly.

In order to utilize the strain sensing and actuating properties of piezoelectric materials, the interaction between the structure and the intelligent material must be well understood. Mechanical models for studying the interaction of piezoelectric patches surface mounted to plates have been developed by a number of investigators. To name a few, Lee (1990) derived a theory for laminated piezoelectric plates, where the linear piezoelectric constitutive equations were the only source of coupling between the electric field and the mechanical displacement field. Tiersten (1969) modeled single layer piezoelectric plates, including the charge equations, but did not study laminates. Tauchert (1992) presented a theory for laminated piezoelectric plates including the thermal effects. These studies are all based on the classical plate theory. To begin addressing the influence of transverse shear effects on smart piezoelectric composite plates subjected to mechanical or thermal loads, Jonnalagadda *et al.* (1994) developed a theory for laminated piezoelectric plates used a Reissner-Mindlin or first order shear deformation theory. Analytical and finite element solutions for plates having simply supported or fixed boundary conditions are presented. Then various kinds of refined higher order shear deformation theories for laminated piezoelectric plates have been developed by Fernandes (2001), Mitchell and Reddy (1995). All the theories mentioned above are based on an assumption that the distribution of electrostatic potential through thickness is linear or a fixed known function of coordinate z. This is not in accordance with the actual case, and the numerical results are not with enough accuracy. Recently, exact three-dimensional solutions for this problem are carried out by several investigators employing different method, see Heyliger (1991, 1996, 1997), Bisegna (1996), Jong (1996), Chen (1997) and *et al.* It is no doubt that these theories can generate excellent results, however, the computational costs will be very high. To generate moderately accuracy solutions with little computational efforts, the present paper provides an analytical solution for a four edges grounded piezoelectric sandwich plate with simply supported mechanical boundary conditions base on the first order shear deformation theory. In our studies, no assumptions are made to the electric potential in any directions of the plate.

2. Basic equations

Generally, the constitutive relations for piezoelectric materials are as follows

$$\sigma = c\varepsilon - e^T E, \quad D = e\varepsilon + gE \tag{1}$$

where, D and E are the electrical displacements vector and the applied electric field intensity vector respectively; σ and ε are the stress vector and strain vector respectively; c, e and g are the elastic coefficients matrix, the piezoelectric stress coefficients matrix and the dielectric permittivity matrix respectively. For an isotropic piezoelectric material polarized in z direction, these matrixes are

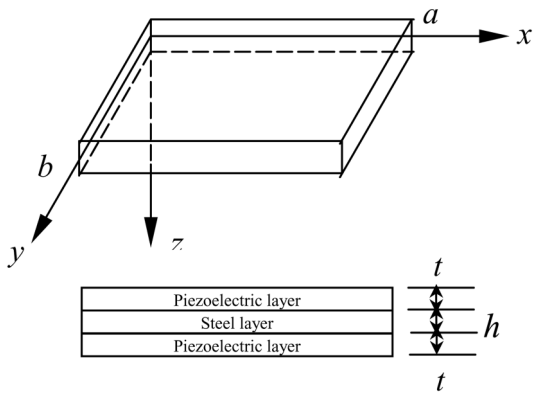

Fig. 1 Geometric and laminate configurations

$$c = \begin{bmatrix} c_{11} & c_{12} & c_{13} & 0 & 0 & 0 \\ c_{12} & c_{22} & c_{23} & 0 & 0 & 0 \\ c_{13} & c_{23} & c_{33} & 0 & 0 & 0 \\ 0 & 0 & 0 & c_{44} & 0 & 0 \\ 0 & 0 & 0 & 0 & c_{55} & 0 \\ 0 & 0 & 0 & 0 & 0 & c_{66} \end{bmatrix}, \quad e^T = \begin{bmatrix} 0 & 0 & e_{31} \\ 0 & 0 & e_{32} \\ 0 & 0 & e_{33} \\ 0 & e_{24} & 0 \\ e_{15} & 0 & 0 \\ 0 & 0 & 0 \end{bmatrix}, \quad g = \begin{bmatrix} g_{11} & 0 & 0 \\ 0 & g_{22} & 0 \\ 0 & 0 & g_{33} \end{bmatrix} \tag{2}$$

where $c_{11} = c_{22}$, $c_{13} = c_{23}$, $c_{44} = c_{55}$, $c_{66} = (c_{11} - c_{12})/2$, $g_{11} = g_{22}$, $e_{15} = e_{24}$, $e_{31} = e_{32}$.

The stress equations of equilibrium and the equation of electrostatics are as follows

$$\sigma_{ij,j} + X_i = 0, \quad D_{i,i} = 0 \tag{3}$$

where $X_i (i = 1, 2, 3)$ are the applied volume force density components. The strains are expressed in terms of the displacements u_i, and the electric field intensities E_i are expressed by an electric potential function Φ as

$$\varepsilon_{ij} = \frac{1}{2}(u_{i,j} + u_{j,i}), \quad E_i = -\Phi_{,i} \tag{4}$$

Consider an isotropic rectangular plate mounted with two piezoelectric layers on the bottom and top surfaces. The geometric shape and the coordinate system of the plate are shown in Fig. 1. The length and width of the plate is a and b respectively. The thickness of the elastic layer and two piezoelectric layers is h and t respectively.

Consistent with first order shear deformation theory, the displacement components are taken to be of the form

$$u_1 = -z\alpha, \quad u_2 = -z\beta, \quad u_3 = w \tag{5}$$

where α and β are the rotations about x and y axes respectively. Using the displacements of Eqs. (5), the strains are given by

$$\varepsilon_x = -z\frac{\partial \alpha}{\partial x}, \quad \varepsilon_y = -z\frac{\partial \beta}{\partial y}, \quad \varepsilon_z = 0, \quad \gamma_{yz} = -\beta + \frac{\partial w}{\partial y}, \quad \gamma_{zx} = -\alpha + \frac{\partial w}{\partial x}, \quad \gamma_{xy} = -z\left(\frac{\partial \alpha}{\partial y} + \frac{\partial \beta}{\partial x}\right) \tag{6}$$

Integrating the constitutive relationships of Eqs. (1) through the composite plate thickness leads to the structure material stiffness relationships. The bending stiffness and the shear stiffness coefficients are given as

$$A_x = \sum_{i=1}^{3}\int_{h_i}^{h_{i+1}} z^2 c_{11}^{(i)} dz, \quad A_y = \sum_{i=1}^{3}\int_{h_i}^{h_{i+1}} z^2 c_{12}^{(i)} dz, \quad G = \sum_{i=1}^{3}\int_{h_i}^{h_{i+1}} c_{44}^{(i)} dz \tag{7}$$

The bending moments, twisting moments and the shear force resultants are written as

$$M_x = -\left(A_x\frac{\partial\alpha}{\partial x} + A_y\frac{\partial\beta}{\partial y}\right) + 2\int_{h/2}^{h/2+t} z e_{31}\frac{\partial\Phi}{\partial z}dz, \quad M_y = -\left(A_y\frac{\partial\alpha}{\partial x} + A_x\frac{\partial\beta}{\partial y}\right) + 2\int_{h/2}^{h/2+t} z e_{32}\frac{\partial\Phi}{\partial z}dz$$

$$M_{xy} = -\frac{A_x - A_y}{2}\left(\frac{\partial\alpha}{\partial y} + \frac{\partial\beta}{\partial x}\right), \quad Q_x = G\left(-\alpha + \frac{\partial w}{\partial x}\right) + 2\int_{h/2}^{h/2+t} e_{15}\frac{\partial\Phi}{\partial x}dz \tag{8}$$

$$Q_y = G\left(-\beta + \frac{\partial w}{\partial y}\right) + 2\int_{h/2}^{h/2+t} e_{24}\frac{\partial\Phi}{\partial y}dz$$

Substituting Eqs. (8) into the three equations of equilibrium

$$\begin{aligned} \frac{\partial M_x}{\partial x} + \frac{\partial M_{yx}}{\partial y} - Q_x &= 0 \\ \frac{\partial M_{xy}}{\partial x} + \frac{\partial M_y}{\partial y} - Q_y &= 0 \\ \frac{\partial Q_x}{\partial x} + \frac{\partial Q_y}{\partial y} + q &= 0 \end{aligned} \tag{9}$$

and substituting the second equation of Eqs. (1) into the second equation of Eqs. (3), one can obtain the governing equations of the problem

$$\begin{aligned} &A_x\frac{\partial^2\alpha}{\partial x^2} + \frac{A_x - A_y}{2}\frac{\partial^2\alpha}{\partial y^2} - G\alpha + \frac{A_x + A_y}{2}\frac{\partial^2\beta}{\partial x\partial y} + G\frac{\partial w}{\partial x} - 2\int_{h/2}^{h/2+t} z e_{31}\frac{\partial^2\Phi}{\partial x\partial z}dz + 2\int_{h/2}^{h/2+t} e_{15}\frac{\partial\Phi}{\partial x}dz = 0 \\ &\frac{A_x + A_y}{2}\frac{\partial^2\alpha}{\partial x\partial y} + \frac{A_x - A_y}{2}\frac{\partial^2\beta}{\partial x^2} - G\beta + A_x\frac{\partial^2\beta}{\partial y^2} + G\frac{\partial w}{\partial y} - 2\int_{h/2}^{h/2+t} z e_{32}\frac{\partial^2\Phi}{\partial y\partial z}dz + 2\int_{h/2}^{h/2+t} e_{24}\frac{\partial\Phi}{\partial y}dz = 0 \\ &G\left(\frac{\partial\alpha}{\partial x} + \frac{\partial\beta}{\partial y} - \frac{\partial^2 w}{\partial x^2} - \frac{\partial^2 w}{\partial y^2}\right) - 2e_{15}\int_{h/2}^{h/2+t}\nabla^2\Phi dz - q = 0 \\ &g_{11}\frac{\partial^2\Phi}{\partial x^2} + g_{22}\frac{\partial^2\Phi}{\partial y^2} + g_{33}\frac{\partial^2\Phi}{\partial z^2} + (e_{15} + e_{31})\frac{\partial\alpha}{\partial x} + (e_{24} + e_{32})\frac{\partial\beta}{\partial y} - e_{15}\frac{\partial^2 w}{\partial x^2} - e_{24}\frac{\partial^2 w}{\partial y^2} = 0 \end{aligned} \tag{10}$$

Suppose the four edges of the plate are grounded, the charge boundary conditions along four edges can be written as

$$\Phi = 0 \tag{11}$$

When the top surface of the plate is applied with external voltage, the charge boundary conditions are expressed as

$$z = h/2 : D_z = 0; \quad z = (h/2 + t) : \Phi = \Phi_0(x, y) \tag{12}$$

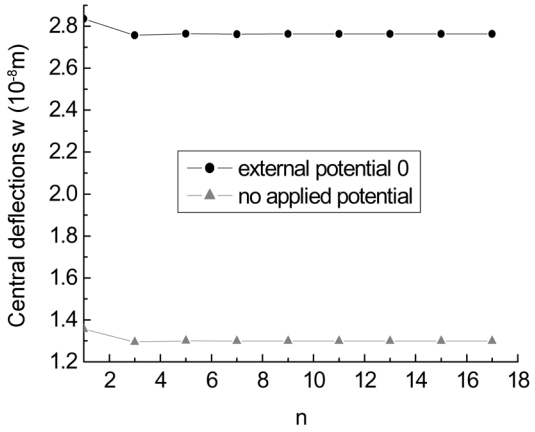

Fig. 2 Convergence characteristic of central deflection of the plate applied with uniform loading $q = 1000$ kN/m^2

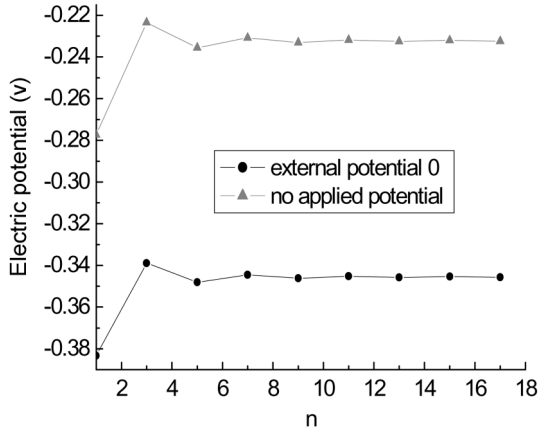

Fig. 3 Convergence characteristic of electrostatic potential at the central point of the plate applied with uniform loading $q = 1000$ kN/m^2

where $\Phi_0(x, y)$ is the applied external potential on top surface of the plate. When the surface of the plate is applied only with a uniform transverse load and with no external voltage, the charge boundary conditions should be expressed as

$$z = h/2 : D_z = 0; \quad z = (h/2 + t) : D_z = 0 \tag{13}$$

According to the first order shear deformation theory, the mechanical boundary conditions for simply supported edges are as follows

$$x = 0,\ a : M_x = 0,\ w = 0,\ \beta = 0;\ y = 0,\ b : M_y = 0, w = 0, \alpha = 0 \tag{14}$$

3. Method of solution

For boundary conditions imposed in Eqs. (11) to (14), the solution to the displacement equations of equilibrium can be expressed in the Fourier's series form

$$\begin{aligned}
\alpha(x, y) &= \sum_{i,j=1}^{\infty} \alpha_{ij} \cos\frac{i\pi x}{a} \sin\frac{j\pi y}{b} \\
\beta(x, y) &= \sum_{i,j=1}^{\infty} \beta_{ij} \sin\frac{i\pi x}{a} \cos\frac{j\pi y}{b} \\
w(x, y) &= \sum_{i,j=1}^{\infty} w_{ij} \sin\frac{i\pi x}{a} \sin\frac{j\pi y}{b} \\
\Phi(x, y, z) &= \sum_{i,j=1}^{\infty} \Phi_{ij}(z) \sin\frac{i\pi x}{a} \sin\frac{j\pi y}{b}
\end{aligned} \tag{15}$$

which seem satisfying the boundary conditions (11) and (14) along four edges. For boundary conditions (12) and (13) on the two surfaces, we can rewrite them by substituting Eqs. (15) into Eqs. (1) then into Eqs. (12) and (13) as follows

$$z = h/2: \quad \begin{aligned} D_z &= ze_{31}\left(\frac{i\pi}{a}\right)\sum_{i=1}^{\infty}\sum_{j=1}^{\infty}\alpha_{ij}\sin\left(\frac{i\pi x}{a}\right)\sin\left(\frac{j\pi y}{b}\right) \\ &+ze_{32}\left(\frac{j\pi}{b}\right)\sum_{i=1}^{\infty}\sum_{j=1}^{\infty}\beta_{ij}\sin\left(\frac{i\pi x}{a}\right)\sin\left(\frac{j\pi y}{b}\right) - g_{33}\sum_{i=1}^{\infty}\sum_{j=1}^{\infty}\frac{\mathrm{d}\Phi_{ij}}{\mathrm{d}z}\sin\left(\frac{i\pi x}{a}\right)\sin\left(\frac{j\pi y}{b}\right) = 0 \end{aligned}$$

$$z = (h/2 + t): \Phi = \sum_{i=1}^{\infty}\sum_{j=1}^{\infty}\Phi_{ij}\sin\left(\frac{i\pi x}{a}\right)\sin\left(\frac{j\pi y}{b}\right) = \sum_{i=1}^{\infty}\sum_{j=1}^{\infty}\Phi_{0ij}\sin\left(\frac{i\pi x}{a}\right)\sin\left(\frac{j\pi y}{b}\right) \tag{16}$$

and

$$z = h/2, \quad z = (h/2 + t): \quad \begin{aligned} D_z &= ze_{31}\left(\frac{i\pi}{a}\right)\sum_{i=1}^{\infty}\sum_{j=1}^{\infty}\alpha_{ij}\sin\left(\frac{i\pi x}{a}\right)\sin\left(\frac{j\pi y}{b}\right) \\ &+ze_{32}\left(\frac{i\pi}{b}\right)\sum_{i=1}^{\infty}\sum_{j=1}^{\infty}\beta_{ij}\sin\left(\frac{i\pi x}{a}\right)\sin\left(\frac{j\pi y}{b}\right) - g_{33}\sum_{i=1}^{\infty}\sum_{j=1}^{\infty}\frac{\mathrm{d}\Phi_{ij}}{\mathrm{d}z}\sin\left(\frac{i\pi x}{a}\right)\sin\left(\frac{j\pi y}{b}\right) = 0 \end{aligned} \tag{17}$$

where Φ_{0ij} is the coefficients of the Fourier's series for applied voltage Φ_0. Substituting Eqs. (15) into the forth equation of Eqs. (10), we obtain

$$\frac{\mathrm{d}^2\Phi_{ij}}{\mathrm{d}z^2} - \omega_{ij}^2\Phi_{ij} + \theta_{ij}^2 = 0 \tag{18}$$

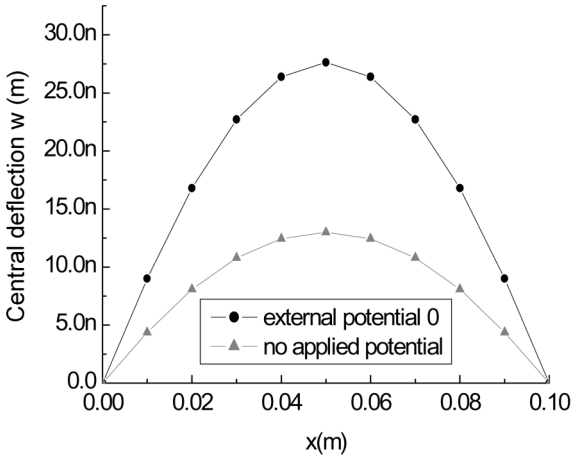

Fig 4 Distribution of deflections for plate under uniform load $q = 1000$ kN/m^2

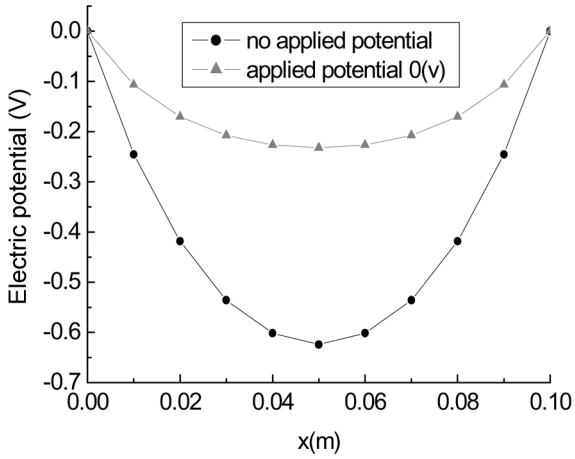

Fig. 5 Distribution of electrostatic potentials on the bottom face of the top layer for plate under uniform load $q = 1000$ kN/m^2 ($y = 0.05$ m)

where

$$\omega_{ij}^2 = \frac{g_{11}\left(\frac{i\pi}{a}\right)^2 + g_{22}\left(\frac{j\pi}{b}\right)^2}{g_{33}} \tag{19}$$

$$\theta_{ij}^2 = \frac{e_{15}\left[\left(\frac{i\pi}{a}\right)^2 + \left(\frac{j\pi}{b}\right)^2\right]w_{ij} - \frac{i\pi}{a}(e_{15} + e_{31})\alpha_{ij} - \frac{j\pi}{b}(e_{24} + e_{32})\beta_{ij}}{g_{33}} \tag{20}$$

The general form for solution of Eq. (18) can be written as

$$\Phi_{ij} = A\sinh\omega_{ij}z + B\cosh\omega_{ij}z + \theta_{ij}^2/\omega_{ij}^2 \tag{21}$$

in which the integrating coefficients A and B are determined by the top and bottom surface charge boundary conditions (16) and (17).

When the external voltage $\Phi_0(x, y)$ is applied on the top surface, Eq. (21) can be rewritten as

$$\Phi_{ij} = \frac{h\left(e_{31}\frac{i\pi}{a}\alpha_{ij} + e_{32}\frac{j\pi}{b}\beta_{ij}\right)}{2g_{33}\omega_{ij}\cosh\omega_{ij}t}\sinh\omega_{ij}\left(z - \frac{h}{2} - t\right) + \frac{\Phi_{0ij} - \theta_{ij}^2/\omega_{ij}^2}{\cosh\omega_{ij}t}\cosh\omega_{ij}\left(z - \frac{h}{2}\right) + \theta_{ij}^2/\omega_{ij}^2 \tag{22}$$

which satisfying boundary conditions (16). Substituting Eq. (22) and Eqs. (15) into the first three equations of Eqs. (10), we obtain the following linear algebraic equations about α_{ij}, β_{ij} and w_{ij}.

$$\begin{aligned}
\mu_{11}\alpha_{ij} + \mu_{12}\beta_{ij} + \mu_{13}w_{ij} + \mu_{14} &= 0 \\
\mu_{21}\alpha_{ij} + \mu_{22}\beta_{ij} + \mu_{23}w_{ij} + \mu_{24} &= 0 \\
\mu_{31}\alpha_{ij} + \mu_{32}\beta_{ij} + \mu_{33}w_{ij} + \mu_{34} &= 0
\end{aligned} \tag{23}$$

where the coefficients $\mu_{st}(s = 1, 2, 3;\ t = 1, 2, 3, 4)$ are expressed in appendix I.

When the surface of the plate is applied with only external mechanical load, the solution of Eq. (18) satisfying boundary conditions (17) can be expressed as

$$\Phi_{ij} = \frac{e_{31}\frac{i\pi}{a}\alpha_{ij} + e_{32}\frac{j\pi}{b}\beta_{ij}}{g_{33}\omega_{ij}\sinh\omega_{ij}t}\left[\left(\frac{h}{2} + t\right)\cosh\omega_{ij}\left(z - \frac{h}{2}\right) - \frac{h}{2}\cosh\omega_{ij}\left(z - \frac{h}{2} - t\right)\right] + \theta_{ij}^2/\omega_{ij}^2 \tag{24}$$

Similarly, substituting this equation and Eqs. (15) into the first three equations of Eqs. (10), we can also obtain a set of linear algebraic equations about α_{ij}, β_{ij} and w_{ij} as Eqs. (23). Here the coefficients $\mu_{st}(s = 1, 2, 3;\ t = 1, 2, 3, 4)$ are expressed in appendix II.

Solving the linear algebraic Eqs. (23), one can obtain the Fourier coefficients of rotations and deflections. Then substituting these coefficients into Eqs. (22) or (24), the Fourier series coefficients of the electric potential function can be obtained.

4. Results and discussion

In this section, the response of a simply supported square sandwich piezoelectric plate subjected to mechanical and electric field loading is carried out. The length and width of the plate is $a = b = 0.1$. The plate is constructed with three laminates, PVDF/steel/PVDF. The thickness of the elastic layer and the piezoelectric layer is $h = 0.01$, $t = h/4$, respectively. Material properties for PVDF layer are $E = 2.0 \times 10^9$ N/m^2; $e_{31} = e_{32} = 0.0483$ C/m^2; $e_{33} = -0.072$ C/m^2; $e_{15} = e_{24} = -0.04$ C/m^2. $g_{11} = g_{22} = g_{33} = 1.062 \times 10^{-10}$ F/m. Properties for steel laminae are $E = 2.1 \times 10^{11}$ N/m^2; $\nu = 0.3$. In order to determine the number of Fourier's series required for resulting solutions with high accuracy, convergency studies are carried out firstly. Fig. 2 demonstrates the convergence pattern of center point deflections of the plate under uniform loading condition $q = 1000$ N/m^2 and applied with 0(V) electric potential or no electric potential on top surface of the plate. It is observed that the deflections are converged to stable values with increasing the number of Fourier series n. The convergence demonstrates a slight fluctuation characteristic. It is easily found that only 5 orders of Fourier's series are needed to obtain the deflection solutions with acceptable accuracy. One can also found that the numerical values of deflections for plate applied with 0(v) external electric voltage on top surface are 2 times greater than those for plate with no external voltage. This means that the effect of electric potential on deflections due to the piezoelectric coupling is very high. The convergence properties of electric potentials at the center point on the bottom surface of the top piezoelectric layer are shown in Fig. 3. It is evident that the convergence of electrostatic potential also demonstrates a fluctuation property; however, the convergence rate is much slower than that of deflections as shown in Fig. 2. Generally speaking, 10 orders of Fourier's series can give good results for all cases considered in this paper. In all the following studies, 15 items of sine or cosine series are employed to acquire solutions with higher accuracy.

Base on the convergence studies, we calculate the deflections and electrostatic potentials of a piezoelectric plate with four edges grounded charge boundary conditions and simply supported

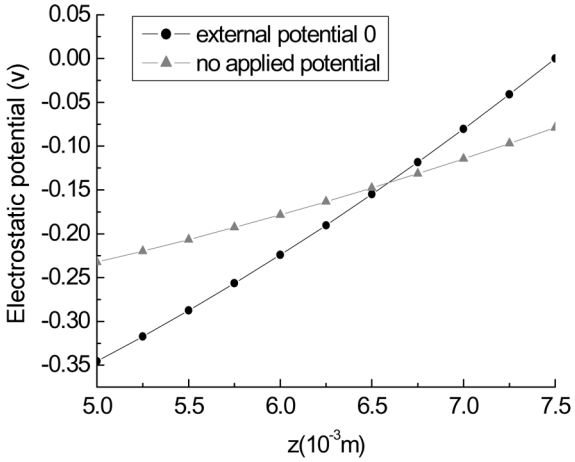

Fig. 6 Electric potential at the central point through thickness of the plate applied with uniform loading $q = 1000$ kN/m^2

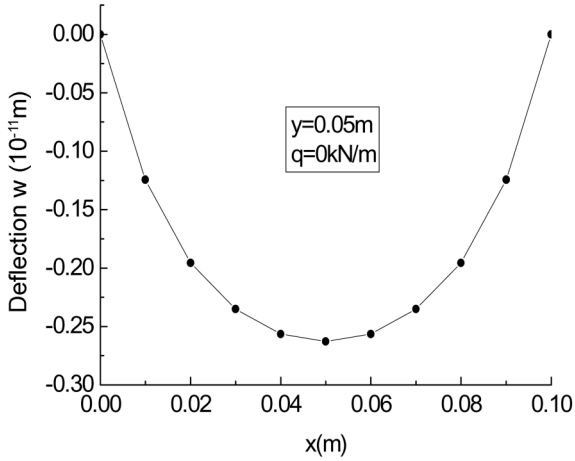

Fig. 7 Deflections of the plate applied with uniform external unit potential on top surface of the plate

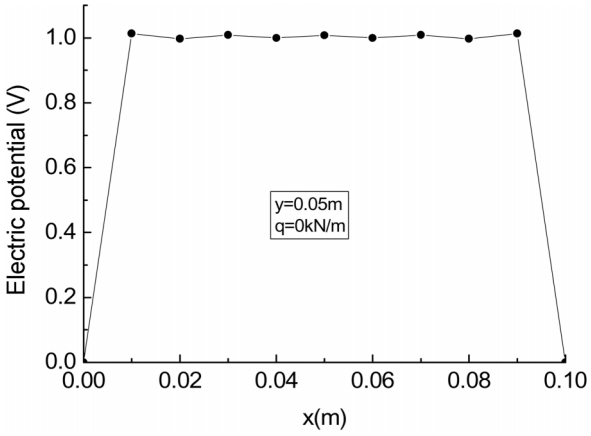

Fig. 8 Electrostatic potentials on the bottom face of the top layer under uniform external unit potential

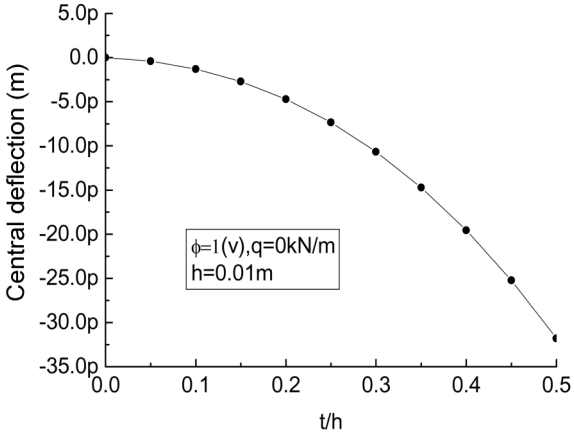

Fig. 9 Influence of the relative thickness ratio of piezoelectric layer to steel layer on central deflections

mechanical boundary conditions. Figs. 4 and 5 demonstrate the distribution of deflections and potentials of the plate subjected to a uniform distributed mechanical load $q = 1000$ N/m^2 and applied with 0(V) external potential as well as with no external potential on the top surface. It is seen from these two figures that the deflections and the electrostatic potentials vary in a parabolic manner in the plate in-plane directions. It is evident that the values of displacements and electric potentials in case 0(v) external potential applied is much higher than those in case no external potential applied. Fig. 6 illustrates the distribution of electrostatic potential through thickness at the central point of the plate applied with uniform loading $q = 1000$ N/m^2. Also, two electric conditions, 0(v) external potential and no external potential applied are considered. It is obvious that the electrostatic potential is almost linear in the thickness direction. These numerical results ascertain the rationality of the linear electric potential assumption through thickness some researchers employed. It is also found that the difference of electric potential between two surfaces of the top layer is much higher for plate applied with 0(v) external voltage than for plate applied with no external voltage.

Figs. 7 and 8 are the distribution diagrams of the central deflections and the electrostatic potentials on bottom surface of the top layer when the plate is applied only with a unit uniform potential on top surface of the top surface. We can see from Fig. 7 that the displacements produced by external potential also show a parabola diagram along the x-axis, just like the distribution diagram of displacements produced by mechanic load showed in Fig. 4. The electrostatic potentials however, are found from Fig. 8 that demonstrate a constant line in this loading case except for the two points at the edge. In Fig. 9, the effect of piezoelectric thickness ratio t/h on the deflections at center point produced by a unit potential is plotted. It is easy to find that the deflection at center point increases monotonically as the piezoelectric thickness ratio increases from 0 to 0.5.

At last, comparison studies are made to verify the accuracy of the present method. In comparison studies, the material properties are identical as in the previous studies except for e_{15} and e_{23} which are chosen as 0. The plate is also in the same form of geometric shape as in the previous studies. Figs. 10 and 11 plot the results of deflections and electric potentials respectively, which are generated by the classical plate theory (Zhang 2000) and by the present first order shear deformation theory. One can easily find that the present results are in good agreement with Zhang's

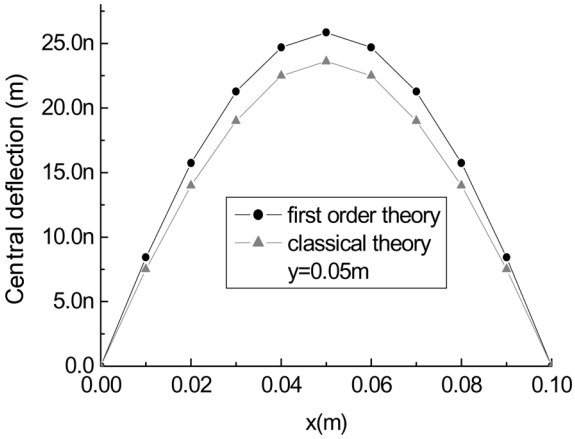

Fig. 10 Comparison of central deflections of the plate under uniform load q = 1000 kN/m (ϕ = 0 on top face)

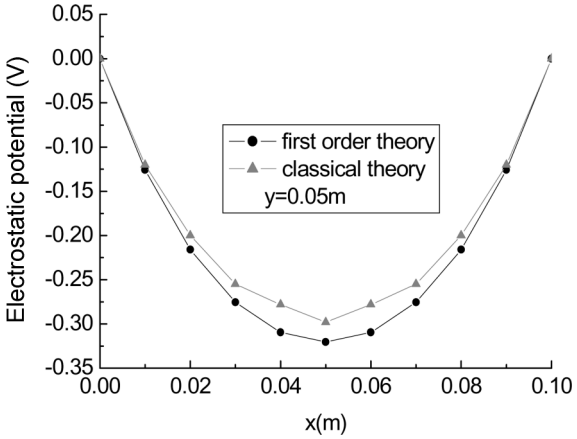

Fig. 11 Comparison of electrostatic potentials on bottom surface of the plate under uniform load q = 1000 kN/m (ϕ = 0 on top face)

results. The present results are higher than those calculated by Zhang *et al.* using the classical plate theory. The maximum discrepancy of deflections between two results is 10.8%, and the maximum discrepancy of electric potentials is 6.8%. We should note that the classical plate theory always generates lower results than the first order shear deformation theory in general, since it makes the plate stiffness much higher.

5. Conclusions

This paper presents an analytical model for a sandwich piezoelectric plate based on the first order shear deformation theory. The governing equations and boundary conditions including the equilibrium equation and charge equation of the plate subjected to a uniformly distributed mechanical load are derived firstly. Then an analytical solution to the problem is presented by Fourier series expansion. Convergency and comparison studies show that the deflections and potentials converge to stable values with high accuracy when increasing the number of Fourier series, and the convergence rate of the present method is very fast. Numerical results demonstrate that the deflections and the electrostatic potentials are distributed in a parabolic manner in the plate in-plane directions, while the electrostatic potentials are distributed linearly in the thickness direction. From these numerical results we can conclude that the influence of electric potentials on the deflections of the plate is considerable high, and cannot be neglected especially as the thickness of piezoelectric layer is not so small. These results can also be used as a benchmark to verify the accuracy of other numerical results.

The present model is valid only for a symmetric sandwich plate, and cannot be used to a non-symmetric multi layered plate.

References

Bisegna, P. and Maccri, F. (1996), "An exact three-dimensional solution for simply supported rectangular piezoelectric plates", *J. Appl. Mech.*, ASME, **63**, 628-637.

Chandrashekhara, K. and Agarwal, A.N. (1993), "Active vibration control of laminated composite plates using piezoelectric devices: a finite element approach", *J. Intelligent Mater. Sys. Struct.*, **4**, 496-508.

Chen, W.Q. and Ding, H.J. (1997), "Three dimensional analysis of bending problem of thick piezoelectric composite rectangular plates", *Acta Materae Compositae Sinica*, **14**, 108-115(in Chinese).

Fernandes, A. and Pouget, J. (2001), "Two-dimensional modeling of laminated piezoelectric composites: analysis and numerical results", *Thin Walled Structures*, **39**, 3-22.

Heyliger, P. (1991), "Static behavior of laminated elastic/piezoelectric plates", *AIAA Journal*, **32**, 2481-2484.

Heyliger, P. and Brooks, S. (1996), "Exact solutions for laminated piezoelectric plates in cylindrical bending", *J. Appl. Mech.*, ASME, **63**, 903-907.

Heyliger, P. (1997), "Exact solutions for simply supported laminated piezoelectric plates", *J. Appl. Mech.*, ASME, **64**, 299-306.

Jong, S.L. and Long, Z.J. (1996), "Exact electric analysis of piezoelectric; laminae via state space approach", *Int. J. Solids Struct.*, **33**, 977-990.

Jonnalagadda, K.D., Blandford, G.E. and Tauchert, T.R. (1994), "Piezothermoelastic composite plate analysis using first-order shear deformation theory", *Comput. Struct.*, **51**, 79-89.

Lee, C.K. (1990), "Theory of laminated piezoelectric plates for the design of distributed sensors/actuators: part I: governing equations and reciprocal relationships", *J. Acoustical Soc. Amer.*, **87**, 1144-1158.

Mitchell, J.A. and Reddy, J.N. (1995), "A refined hybrid plate theory for composite laminates with piezoelectric laminar", *Int. J. Solids Struct.*, **32**, 2345-2367.

Tauchert, T.R. (1992), "Piezothermoelastic behavior of a laminate", *J. Thermal Stresses*, **15**, 25-37.

Tiersten, H.F. (1969), *Linear Piezoelectric Plate Vibrations*, Plenum Publications, Newyork.

Zhang, J.G., Liu, Zhengxing and Lin, Qirong (2000), "An analytical solution for static electromechanical coupled behavior of a laminated piezoelectric plate", *Acta Mechnica Sinica*, **32**(3), 326-333(in Chinese).

Appendix I: Coefficients μ_{st} in case that external voltage is applied in the top surface of the plate

$$\mu_{11} = -A_x\left(\frac{i\pi}{a}\right)^2 - \frac{A_x - A_y}{2}\left(\frac{j\pi}{b}\right)^2 - G - \frac{e_{31}^2 h(-2 + 2\cosh\omega_{ij}t + \omega_{ij}h\sinh\omega_{ij}t)}{2\omega_{ij}^2 g_{33}\cosh\omega_{ij}t}\left(\frac{i\pi}{a}\right)^2$$

$$+ \frac{e_{31}e_{15}h(1-\cosh\omega_{ij}t)}{g_{33}\omega_{ij}^2\cosh\omega_{ij}t}\left(\frac{i\pi}{a}\right)^2 + \frac{2(e_{31}e_{15} + e_{15}^2)}{g_{33}\omega_{ij}^3\cosh\omega_{ij}t}\left(\frac{i\pi}{a}\right)^2\sinh\omega_{ij}t - \frac{2(e_{15}^2 + e_{15}e_{31})t}{g_{33}\omega_{ij}^2}\left(\frac{i\pi}{a}\right)^2$$

$$-\frac{2(e_{31}e_{15} + e_{31}^2)}{g_{33}\omega_{ij}^3\cosh\omega_{ij}t}\left[\left(\frac{h}{2} + t\right)\omega_{ij}\cosh\omega_{ij}t - \frac{h}{2}\omega_{ij} - \sinh\omega_{ij}t\right]\left(\frac{i\pi}{a}\right)^2,$$

$$\mu_{12} = -\frac{A_x + A_y}{2}\left(\frac{i\pi}{a}\right)\left(\frac{j\pi}{b}\right) - \frac{e_{31}e_{32}h(-2 + 2\cosh\omega_{ij}t + \omega_{ij}h\sinh\omega_{ij}t)}{2\omega_{ij}^2 g_{33}\cosh\omega_{ij}t}\left(\frac{i\pi}{a}\right)\left(\frac{j\pi}{b}\right)$$

$$-\frac{2e_{31}(e_{24} + e_{32})}{g_{33}\omega_{ij}^3\cosh\omega_{ij}t}\left[\left(\frac{h}{2} + t\right)\omega_{ij}\cosh\omega_{ij}t - \frac{h}{2}\omega_{ij} - \sinh\omega_{ij}t\right]\left(\frac{i\pi}{a}\right)\left(\frac{j\pi}{b}\right)$$

$$+ \frac{e_{32}e_{15}h(1-\cosh\omega_{ij}t)}{g_{33}\omega_{ij}^2\cosh\omega_{ij}t}\left(\frac{i\pi}{a}\right)\left(\frac{j\pi}{b}\right) + \frac{2(e_{24} + e_{32})e_{15}}{g_{33}\omega_{ij}^3\cosh\omega_{ij}t}\left(\frac{i\pi}{a}\right)\left(\frac{j\pi}{b}\right)\sinh\omega_{ij}t$$

$$-\frac{2e_{15}(e_{32}+e_{24})t}{g_{33}\omega_{ij}^2}\left(\frac{i\pi}{a}\right)\left(\frac{j\pi}{b}\right),$$

$$\mu_{13} = G\left(\frac{i\pi}{a}\right)+\frac{2e_{31}e_{15}}{g_{33}\omega_{ij}^3\cosh\omega_{ij}t}\left(\frac{i\pi}{a}\right)\left[\left(\frac{i\pi}{a}\right)^2+\left(\frac{j\pi}{b}\right)^2\right]\left[\left(\frac{h}{2}+t\right)\omega_{ij}\cosh\omega_{ij}t-\frac{h}{2}\omega_{ij}-\sinh\omega_{ij}t\right]$$

$$-\frac{2e_{15}^2}{g_{33}\omega_{ij}^3\cosh\omega_{ij}t}\left(\frac{i\pi}{a}\right)\left[\left(\frac{i\pi}{a}\right)^2+\left(\frac{j\pi}{b}\right)^2\right]\sinh\omega_{ij}t+\frac{2e_{15}^2t}{g_{33}\omega_{ij}^2}\left(\frac{i\pi}{a}\right)\left[\left(\frac{i\pi}{a}\right)^2+\left(\frac{j\pi}{b}\right)^2\right],$$

$$\mu_{14} = -\frac{e_{31}\Phi_{0ij}}{\omega_{ij}\cosh\omega_{ij}t}\left(\frac{i\pi}{a}\right)(-2+2\cosh\omega_{ij}t+\omega_{ij}h\sinh\omega_{ij}t)+\frac{2e_{15}\Phi_{0ij}}{\omega_{ij}\cosh\omega_{ij}t}\left(\frac{i\pi}{a}\right)\sinh\omega_{ij}t,$$

$$\mu_{21} = -\frac{A_x+A_y}{2}\left(\frac{i\pi}{a}\right)\left(\frac{j\pi}{b}\right)-\frac{e_{31}e_{32}h(-2+2\cosh\omega_{ij}t+\omega_{ij}h\sinh\omega_{ij}t)}{2\omega_{ij}^2g_{33}\cosh\omega_{ij}t}\left(\frac{i\pi}{a}\right)\left(\frac{j\pi}{b}\right)$$

$$-\frac{2e_{32}(e_{15}+e_{31})}{g_{33}\omega_{ij}^3\cosh\omega_{ij}t}\left[\left(\frac{h}{2}+t\right)\omega_{ij}\cosh\omega_{ij}t-\frac{h}{2}\omega_{ij}-\sinh\omega_{ij}t\right]\left(\frac{i\pi}{a}\right)\left(\frac{j\pi}{b}\right)$$

$$+\frac{e_{31}e_{24}h(1-\cosh\omega_{ij}t)}{g_{33}\omega_{ij}^2\cosh\omega_{ij}t}\left(\frac{i\pi}{a}\right)\left(\frac{j\pi}{b}\right)+\frac{2(e_{15}+e_{31})e_{24}}{g_{33}\omega_{ij}^3\cosh\omega_{ij}t}\left(\frac{i\pi}{a}\right)\left(\frac{j\pi}{b}\right)\sinh\omega_{ij}t$$

$$-\frac{2(e_{15}+e_{31})e_{24}t}{g_{33}\omega_{ij}^2}\left(\frac{i\pi}{a}\right)\left(\frac{j\pi}{b}\right),$$

$$\mu_{22} = -A_x\left(\frac{j\pi}{b}\right)^2-\frac{A_x-A_y}{2}\left(\frac{i\pi}{a}\right)^2-G-\frac{e_{32}^2h(-2+2\cosh\omega_{ij}t+\omega_{ij}h\sinh\omega_{ij}t)}{2\omega_{ij}^2g_{33}\cosh\omega_{ij}t}\left(\frac{j\pi}{b}\right)^2$$

$$+\frac{e_{31}e_{24}h(1-\cosh\omega_{ij}t)}{g_{33}\omega_{ij}^2\cosh\omega_{ij}t}\left(\frac{j\pi}{b}\right)^2+\frac{2(e_{32}e_{24}+e_{24}^2)e_{24}}{g_{33}\omega_{ij}^3\cosh\omega_{ij}t}\left(\frac{j\pi}{b}\right)^2\sinh\omega_{ij}t-\frac{2(e_{24}^2+e_{24}e_{32})t}{g_{33}\omega_{ij}^2}\left(\frac{j\pi}{b}\right)^2$$

$$-\frac{2(e_{32}e_{24}+e_{32}^2)}{g_{33}\omega_{ij}^3\cosh\omega_{ij}t}\left[\left(\frac{h}{2}+t\right)\omega_{ij}\cosh\omega_{ij}t-\frac{h}{2}\omega_{ij}-\sinh\omega_{ij}t\right]\left(\frac{j\pi}{b}\right)^2,$$

$$\mu_{23} = G\left(\frac{j\pi}{b}\right)+\frac{2e_{32}e_{15}}{g_{33}\omega_{ij}^3\cosh\omega_{ij}t}\left(\frac{j\pi}{b}\right)\left[\left(\frac{i\pi}{a}\right)^2+\left(\frac{j\pi}{b}\right)^2\right]\left[\left(\frac{h}{2}+t\right)\omega_{ij}\cosh\omega_{ij}t-\frac{h}{2}\omega_{ij}-\sinh\omega_{ij}t\right]$$

$$-\frac{2e_{24}^2}{g_{33}\omega_{ij}^3\cosh\omega_{ij}t}\left(\frac{j\pi}{b}\right)\left[\left(\frac{i\pi}{a}\right)^2+\left(\frac{j\pi}{b}\right)^2\right]\sinh\omega_{ij}t+\frac{2e_{24}^2t}{g_{33}\omega_{ij}^2}\left(\frac{j\pi}{b}\right)\left[\left(\frac{i\pi}{a}\right)^2+\left(\frac{j\pi}{b}\right)^2\right],$$

$$\mu_{24} = -\frac{e_{32}\Phi_{0ij}}{\omega_{ij}\cosh\omega_{ij}t}\left(\frac{j\pi}{b}\right)(-2+2\cosh\omega_{ij}t+\omega_{ij}h\sinh\omega_{ij}t)+\frac{2e_{24}\Phi_{0ij}}{\omega_{ij}\cosh\omega_{ij}t}\left(\frac{j\pi}{b}\right)\sinh\omega_{ij}t,$$

$$\mu_{31} = -G\left(\frac{i\pi}{a}\right)+\frac{e_{31}e_{15}h}{g_{33}\omega_{ij}^2\cosh\omega_{ij}t}\left(\frac{i\pi}{a}\right)\left[\left(\frac{i\pi}{a}\right)^2+\left(\frac{j\pi}{b}\right)^2\right][1-\cosh\omega_{ij}t]$$

$$+\frac{2e_{15}(e_{15}+e_{31})}{g_{33}\omega_{ij}^3\cosh\omega_{ij}t}\left(\frac{i\pi}{a}\right)\left[\left(\frac{i\pi}{a}\right)^2+\left(\frac{j\pi}{b}\right)^2\right]\sinh\omega_{ij}t-\frac{2e_{15}(e_{15}+e_{31})t}{g_{33}\omega_{ij}^2}\left(\frac{i\pi}{a}\right)\left[\left(\frac{i\pi}{a}\right)^2+\left(\frac{j\pi}{b}\right)^2\right],$$

$$\mu_{32} = -G\left(\frac{j\pi}{b}\right)+\frac{e_{32}e_{15}h}{g_{33}\omega_{ij}^2\cosh\omega_{ij}t}\left(\frac{j\pi}{b}\right)\left[\left(\frac{i\pi}{a}\right)^2+\left(\frac{j\pi}{b}\right)^2\right][1-\cosh\omega_{ij}t]$$

$$+\frac{2e_{15}(e_{24}+e_{32})}{g_{33}\omega_{ij}^3\cosh\omega_{ij}t}\left(\frac{j\pi}{b}\right)\left[\left(\frac{i\pi}{a}\right)^2+\left(\frac{j\pi}{b}\right)^2\right]\sinh\omega_{ij}t-\frac{2e_{15}(e_{24}+e_{32})t}{g_{33}\omega_{ij}^2}\left(\frac{j\pi}{b}\right)\left[\left(\frac{i\pi}{a}\right)^2+\left(\frac{j\pi}{b}\right)^2\right],$$

$$\mu_{33}=G\left[\left(\frac{i\pi}{a}\right)^2+\left(\frac{j\pi}{b}\right)^2\right]-\frac{2e_{15}^2}{g_{33}\omega_{ij}^3\cosh\omega_{ij}t}\left[\left(\frac{i\pi}{a}\right)^2+\left(\frac{j\pi}{b}\right)^2\right]^2\sinh\omega_{ij}t$$

$$+\frac{2e_{15}^2t}{g_{33}\omega_{ij}^2}\left[\left(\frac{i\pi}{a}\right)^2+\left(\frac{j\pi}{b}\right)^2\right]^2,$$

$$\mu_{34}=\frac{2e_{15}\Phi_{0ij}}{\omega_{ij}\cosh\omega_{ij}t}\left[\left(\frac{i\pi}{a}\right)^2+\left(\frac{j\pi}{b}\right)^2\right]\sinh\omega_{ij}t-q_{ij}.$$

Appendix II: Coefficients μ_{st} in case that no external voltage is applied

$$\mu_{11}=-A_x\left(\frac{i\pi}{a}\right)^2-\frac{A_x-A_y}{2}\left(\frac{j\pi}{b}\right)^2-G-\frac{2e_{15}t}{\omega_{ij}^2g_{33}}\left(\frac{i\pi}{a}\right)^2$$

$$-2e_{31}^2\frac{\left[\left(\frac{h}{2}+t\right)^2+\left(\frac{h}{2}\right)^2\right]\omega_{ij}\cosh\omega_{ij}t-h\left(\frac{h}{2}+t\right)\omega_{ij}-t\sinh\omega_{ij}t}{\omega_{ij}^2g_{33}\sinh\omega_{ij}t}\left(\frac{i\pi}{a}\right)^2,$$

$$\mu_{12}=-\frac{A_x+A_y}{2}\left(\frac{i\pi}{a}\right)\left(\frac{j\pi}{b}\right)-\frac{2e_{15}e_{24}t}{g_{33}\omega_{ij}^2}\left(\frac{i\pi}{a}\right)\left(\frac{j\pi}{b}\right)$$

$$-2e_{31}e_{32}\frac{\left[\left(\frac{h}{2}+t\right)^2+\left(\frac{h}{2}\right)^2\right]\omega_{ij}\cosh\omega_{ij}t-h\left(\frac{h}{2}+t\right)\omega_{ij}-t\sinh\omega_{ij}t}{\omega_{ij}^2g_{33}\sinh\omega_{ij}t}\left(\frac{i\pi}{a}\right)\left(\frac{j\pi}{b}\right),$$

$$\mu_{13}=G\left(\frac{i\pi}{a}\right)+\frac{2e_{15}^2t}{g_{33}\omega_{ij}^3}\left(\frac{i\pi}{a}\right)\left[\left(\frac{i\pi}{a}\right)^2+\left(\frac{j\pi}{b}\right)^2\right],$$

$$\mu_{21}=-\frac{A_x+A_y}{2}\left(\frac{i\pi}{a}\right)\left(\frac{j\pi}{b}\right)-\frac{2e_{15}e_{24}t}{g_{33}\omega_{ij}^2}\left(\frac{i\pi}{a}\right)\left(\frac{j\pi}{b}\right)$$

$$-2e_{31}e_{32}\frac{\left[\left(\frac{h}{2}+t\right)^2+\left(\frac{h}{2}\right)^2\right]\omega_{ij}\cosh\omega_{ij}t-h\left(\frac{h}{2}+t\right)\omega_{ij}-t\sinh\omega_{ij}t}{\omega_{ij}^2g_{33}\sinh\omega_{ij}t}\left(\frac{i\pi}{a}\right)\left(\frac{j\pi}{b}\right),$$

$$\mu_{22}=-A_x\left(\frac{j\pi}{b}\right)^2-\frac{A_x-A_y}{2}\left(\frac{i\pi}{a}\right)^2-G-\frac{2e_{24}^2t}{g_{33}\omega_{ij}^2}$$

$$-2e_{32}^2\frac{\left[\left(\frac{h}{2}+t\right)^2+\left(\frac{h}{2}\right)^2\right]\omega_{ij}\cosh\omega_{ij}t-h\left(\frac{h}{2}+t\right)\omega_{ij}-t\sinh\omega_{ij}t}{\omega_{ij}^2g_{33}\sinh\omega_{ij}t}\left(\frac{j\pi}{b}\right)^2,$$

$$\mu_{23}=G\left(\frac{j\pi}{b}\right)+\frac{2e_{24}e_{15}t}{g_{33}\omega_{ij}^2}\left(\frac{j\pi}{b}\right)\left[\left(\frac{i\pi}{a}\right)^2+\left(\frac{j\pi}{b}\right)^2\right],$$

$$\mu_{31} = -G\left(\frac{i\pi}{a}\right) - \frac{2e_{15}^2 t}{g_{33}\omega_{ij}^2}\left(\frac{i\pi}{a}\right)\left[\left(\frac{i\pi}{a}\right)^2 + \left(\frac{j\pi}{b}\right)^2\right],$$

$$\mu_{32} = -G\left(\frac{j\pi}{b}\right) - \frac{2e_{15}e_{24}t}{g_{33}\omega_{ij}^2}\left(\frac{j\pi}{b}\right)\left[\left(\frac{i\pi}{a}\right)^2 + \left(\frac{j\pi}{b}\right)^2\right],$$

$$\mu_{33} = G\left[\left(\frac{i\pi}{a}\right)^2 + \left(\frac{j\pi}{b}\right)^2\right] + \frac{2e_{15}^2}{g_{33}\omega_{ij}^2}\left[\left(\frac{i\pi}{a}\right)^2 + \left(\frac{j\pi}{b}\right)^2\right]^2,$$

$$\mu_{14} = 0, \mu_{24} = 0, \mu_{34} = -q_{ij}.$$